A REVIEW OF RECENT STUDY OF GUIDED WAVES IN CHIRAL MEDIA

F. Mariotte, P. Pelet, and N. Engheta

1.   Introduction

In the past several years there has been an increasing interest in understanding fundamental electromagnetic properties of guided waves in complex and composite materials. In particular, analytical and experimental study of guided–wave structures utilizing chiral, and in general bianisotropic materials have recently been the subject of research interest to many researchers and engineers. Chiral materials in general have attracted renewed attention in past several years [1–4]. The interest in wave guiding properties of chiral materials is primarily motivated by the novel and interesting features these waveguiding structures may possess and their possible applications to future design of new devices and components in the optical, microwave, and millimeter wave regimes. It is clear that in general waveguiding elements

constitute an important part of most devices, and as a result the functional characteristics of these devices depend, among many factors, on guidance condition and propagation properties of guided modes in these waveguides. Furthermore, it is well known that guided modes in any structures are affected, among other parameters, by the electromagnetic characteristics of materials used in these structures. This is where the analytical, computational and experimental study of guided waves in complex materials plays an important role. In this chapter, we plan to provide some brief review of recent study of electromagnetic properties of guided waves in chiral materials. The interested readers are referred to a representative sample of articles listed in the bibliography here and the references therein. The reference list is just a representative sample of work in this area, and is, by no means, an exhaustive list.

2.   Review of Basic Formulation

Chiral materials belong to a subset of electromagnetic media known as bianisotropic media [5,6]. These materials are circular polarization birefringent, i.e., the eigenmodes of propagation in these media are right– and left–circularly polarized (RCP and LCP) plane waves [7–9]. These eigenmodes propagate with different phase velocities and possess two unequal wave numbers [7–9]. The time–harmonic constitutive relations governing isotropic reciprocal linear chiral media can be given as

$$\mathbf{D} = \varepsilon_c \mathbf{E} + i\xi_c \mathbf{B} \tag{1a}$$

$$\mathbf{H} = (1/\mu_c)\mathbf{B} + i\xi_c \mathbf{E} \tag{1b}$$

in which the electric and magnetic effects are coupled via a parameter shown as ξ_c and known as chirality admittance [6,8]. The other two parameters ε_c and μ_c are the conventional permittivity and permeability of the medium. The time–harmonic notation of $\exp(i\omega t)$ is assumed here. It must be mentioned that the above constitutive relations are not the only way of describing electromagnetic relations among $\mathbf{E}, \mathbf{B}, \mathbf{D}$, and $\mathbf{H}$ in these media. There are other sets of such relations for chiral media. Two other commonly used sets are: $\mathbf{D} = \varepsilon \ (\mathbf{E} + \beta\nabla \times \mathbf{E})$ and $\mathbf{B} = \mu \ (\mathbf{H} + \beta\nabla \times \mathbf{H})$ where β is the measure of chirality [1,3], and

the other set $D = \varepsilon\,E + i\chi H$ and $B = \mu\,H - i\chi E$ in which χ represents the chirality of the medium [10,11]. Obviously, these sets are physically equivalent, and the parameters in each set can be straightforwardly related to parameters of other set [10,12]. Here in this review chapter, we use the constitutive relation and notations represented in Eq. (1). The results can be easily transformed to other notations using the relationships among these sets of constitutive equations.

In the recent past, there have been several treatments of basic formulation of electromagnetic guided waves in waveguides filled with chiral media. Among these one can mention the work of Engheta and Pelet [13,14], Eftimiu and Pearson [15], Varadan et al. [16], Svedin [17,18], and Hollinger et al. [19] to name a few. The name chirowaveguide was coined to describe guided–wave structures wherein chiral material is used [13,14]. In addition to the basic formulation, subsequent studies on various aspects of chirowaveguides, such as mode coupling, other geometries for chirowaveguides, potential applications, etc. have been carried out by many researchers, and some of these studies will be mentioned and reviewed here shortly. First, we briefly review the basic formulation for the guided waves in homogeneous chiral materials and the relevant results. The details of this analysis can be found in the above references, e.g., in [14].

From a knowledge of chiral constitutive relations of Eq. (1) and the source–free Maxwell equations, it has been shown [9] that the source–free wave equation for the electric field E (as well as the other three field vectors B, D, and H) in homogeneous chiral media can be written as

$$\nabla \times \nabla \times E - 2\omega\mu_c\xi_c\nabla \times E - \omega^2\mu_c\varepsilon_c E = 0 \qquad (2)$$

As is usually done in formulation of guided modes in general cylindrical waveguiding structures [20], the transverse field components can be expressed in terms of the longitudinal field components. Assuming the longitudinal direction (or the waveguide's axis) to be along the z axis in a coordinate system and the guided wave to be propagating in the z direction with propagator $\exp(\gamma z)$ where γ being complex in general [1], the transverse components have been expressed in terms of

----

[1]   The complex wavenumber of γ of a guided mode can be written as $\gamma = i\beta - \alpha$ where β is the propagation constant and α is the attenuation rate of that mode.

E_z and H_z using the Maxwell equations and Eq. (1) [13,14]. They are written as

$$E_t = ia\nabla_t E_z + ibe_z \times \nabla_t H_z + c\nabla_t H_z + de_z \times \nabla_t E_z \qquad (3a)$$

$$H_t = ia\nabla_t H_z - i(b/\eta_c^2)e_z \times \nabla_t E_z - (c/\eta_c^2)\nabla_t E_z + de_z \times \nabla_t H_z \quad (3b)$$

where

$$\nabla_t \equiv \nabla - \partial/\partial z \mathbf{e}_z,$$

$$a \equiv - i\gamma \ \left\{ \left[\left(k_+^2 + k_-^2 \right)/2 \right] + \gamma^2 \right\} / \left[\left(\gamma^2 + k_+^2 \right) \left(\gamma^2 + k_-^2 \right) \right],$$

$$b \equiv - \omega\mu_c \left(\gamma^2 + k^2 \right) / \left[\left(\gamma^2 + k_+^2 \right) \left(\gamma^2 + k_-^2 \right) \right],$$

$$c \equiv - 2i\omega^2\mu_c^2\xi_c\gamma \ / \left[\left(\gamma^2 + k_+^2 \right) \left(\gamma^2 + k_-^2 \right) \right],$$

$$d \equiv \omega\mu_c\xi_c \left(k^2 - \gamma^2 \right) / \left[\left(\gamma^2 + k_+^2 \right) \left(\gamma^2 + k_-^2 \right) \right],$$

with

$$k_\pm = \pm \omega\mu \ \xi_c + \omega\sqrt{\mu_c\varepsilon_c + \mu_c^2\xi_c^2}$$

and

$$k \equiv \omega\sqrt{\mu_c\varepsilon_c}$$
$$\eta_c \equiv 1 \ / \ \sqrt{\varepsilon_c/\mu_c + \xi_c^2}.$$

Combining the source–free wave equation in Eq. (2) with the expressions shown in Eq. (3), it was shown that a set of coupled equations was found for the longitudinal components E_z and H_z [13,14].

$$\nabla_t^2 E_z + \left[\frac{k_+^2 + k_-^2}{2} + \gamma^2 \right] E_z + (2i\omega^2\mu_c^2\xi_c)H_z = 0 \qquad (4a)$$

$$\nabla_t^2 H_z + \left[\frac{k_+^2 + k_-^2}{2} + \gamma^2 \right] H_z - (2i\omega^2\mu_c^2\xi_c/\eta_c^2)E_z = 0 \qquad (4b)$$

It is worth mentioning that up to this step no assumption has been made either on the cross sectional shape of the cylinderical waveguide, on the dispersion characteristics of the chiral materials filling the guide, or on the boundary conditions on the waveguide's walls. It is assumed, however, that guided modes propagate along the waveguide's direction,

i.e., the z axis, the cross-sectional shape is independent of z, and that the medium is homogeneous. [2]

As can be seen from Eq. (4), the two Helmholtz–type differential equations for E_z and H_z (and consequently their corresponding transverse components) are coupled, and the coupling is primarily due to the chirality of the medium, i.e., ξ_c. [3] This is one of the interesting characteristics of chirowaveguides. This suggests that neither E_z nor H_z can be identically zero unless both are zero. If both E_z and H_z are zero, one can show that $\mathbf{E}_t$ and $\mathbf{H}_t$ should also vanish identically. Therefore, no TE, TM, or TEM modes exist individually in a chirowaveguide. If the medium is a simple non–chiral dielectric material, $\xi_c = 0$, and thus the two equations will be decoupled and TE and TM modes can exist [14]. Coupled differential equations of this sort are often encountered in problems of wave propagation in gyrotropic waveguides [22,23]. There are standard mathematical techniques to solve these coupled differential equations. Following a technique similar to that used by Kales for magnetically biased ferrite waveguides [22], the coupled Eqs. (4) were transformed into a new pair of decoupled equations, and then this new set was solved to find expressions for E_z and H_z [14]. Solutions of these equations depend on the geometry of the waveguide and the boundary condition for field components at the waveguide's walls. In the next section, we will review characteristics of guided modes in certain specific chirowaveguide geometries and boundaries.

3.   Metallic Paralle–Plate Chirowaveguides: A Review

The salient features, such as dispersion relations, field distributions, and cutoff frequencies of guided mode propagation in metal-

---

[2] The medium can be transversely or longitudinally piecewise homogeneous. In that case, in each homogeneous region, Eq.(4) can be applied.

[3] The coupling of E_z and H_z mentioned here and in [13,14] is due to the chiral property of the medium. It is also possible that the geometry of the waveguide's boundary would cause couplig between E_z and H_z. A good example of such a boundary is an open dielectric waveguide with elliptical cross section [21].
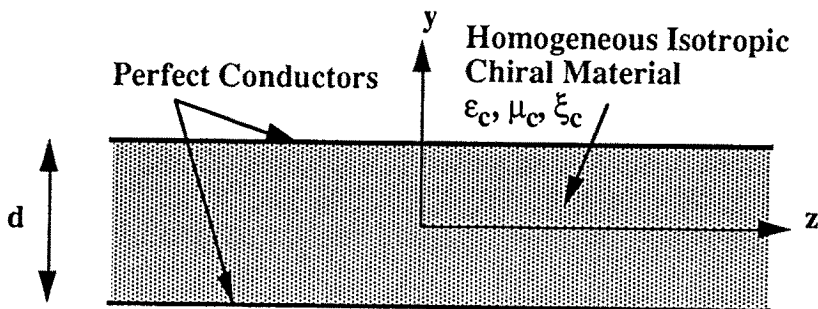
Figure 1. Parallel–plate metallic chirowaveguide with thickness d. The inside region is filled with homogeneous isotropic chiral materials with complex parameters ϵ_c, μ_c, ξ_c.

lic parallel–plate waveguides filled with isotropic lossless homogeneous chiral media were studied and addressed by Pelet and Engheta [14]. The effect of chiral material loss, phenomenologically introduced as the imaginary part of ε_c or μ_c, on characteristics of guided modes in such chirowaveguides were also analyzed by Mariotte and Engheta [24]. Specific detailed analysis was carried out by Mahmoud [25] on the phenomenon of mode bifurcation which was originally introduced by Engheta and Pelet [13,14] and on the characteristics of dominant mode in parallel–plate chirowaveguides. In this section we present a brief overview of some of properties of guided modes in such waveguides.

The geometry of the problem with a Cartesian coordinate system is shown in Fig. 1. Here the direction of propagation is assumed to be in the z direction, and the two perfectly conducting plates, separated by a distance d, are parallel with the $x - z$ plane. The two plates are infinitely extent in both x and z directions. All quantities of interest are independent of x. The region between the two plates is completely filled with a homogeneous, isotropic, reciprocal chiral medium described by the constitutive relations Eq. (1). The boundary conditions on the perfectly conducting walls require the tangential components of electric field vanish on the walls. For the sake of gen-

erality, we assume here that the chiral material is lossy and that all material parameters are, in general complex quantities. The electric field components satisfying the wave equations (2) and (4) and the boundary conditions can be written as follows

$$
E_x = - F_1 \sqrt{\frac{S_1}{S_2}} \left\{ k_+ \sqrt{S_2} \sin(\sqrt{S_1}y) + k_- \sqrt{S_1} \frac{-\cos(\sqrt{S_1}d/2)}{\cos(\sqrt{S_2}d/2)} \sin(\sqrt{S_2}y) \right\}
$$

$$
+ F_2 \sqrt{\frac{S_1}{S_2}} \left\{ k_+ \sqrt{S_2} \cos(\sqrt{S_1}y) + k_- \sqrt{S_1} \frac{-\sin(\sqrt{S_1}d/2)}{\sin(\sqrt{S_2}d/2)} \cos(\sqrt{S_2}y) \right\}
$$

$$
E_y = \gamma F_1 \sqrt{\frac{S_1}{S_2}} \left\{ -\sqrt{S_2} \sin(\sqrt{S_1}y) + \sqrt{S_1} \frac{-\cos(\sqrt{S_1}d/2)}{\cos(\sqrt{S_2}d/2)} \sin(\sqrt{S_2}y) \right\}
$$

$$
+ \gamma F_2 \sqrt{\frac{S_1}{S_2}} \left\{ \sqrt{S_2} \cos(\sqrt{S_1}y) - \sqrt{S_1} \frac{\sin(\sqrt{S_1}d/2)}{\sin(\sqrt{S_2}d/2)} \cos(\sqrt{S_2}y) \right\}
$$

$$
E_z = S_1 F_1 \left\{ \cos(\sqrt{S_1}y) - \frac{\cos(\sqrt{S_1}d/2)}{\cos(\sqrt{S_2}d/2)} \cos(\sqrt{S_2}y) \right\}
$$

$$
+ S_1 F_2 \left\{ \sin(\sqrt{S_1}y) - \frac{\sin(\sqrt{S_1}d/2)}{\sin(\sqrt{S_2}d/2)} \sin(\sqrt{S_2}y) \right\} \tag{5}
$$

where S_1 and S_2 are defined as $S_1 \equiv k_+^2 + \gamma^2$ and $S_2 \equiv k_-^2 + \gamma^2$, with $\gamma \equiv i\beta - \alpha$ being the complex guide wave number of this guided mode with β as the propagation constant and α as the attenuation rate. F_1 and F_2 are two arbitrary coefficients. When F_1 is taken to be zero and $F_2 \neq 0$, the transverse components of electric field are even function of y coordinate, whereas when $F_2 = 0$ and $F_1 \neq 0$, the transverse field components are odd functions of y. The latter is referred to as odd mode, and the former as even mode. [4] The details of the analysis leading to the above results can be found in [14]. The longitudinal component of magnetic field is given as

---

[4] It should be noted that the definition of eveness and oddness for guided modes used in this chapter is different from that used in Refs. [14,26]. Here, the eveness and oddness of modes are chosen based their transverse electric field components, whereas in [14,26] it was defined according to the longitudinal components. So the even (odd) modes here correspond to odd (even) modes described in these references.

$$H_z = \frac{k_+^2 - k_-^2}{4i\omega^2 \mu_c^2 \xi_c} S_1 F_1 \left\{ \cos\left(\sqrt{S_1}y\right) + \frac{\cos\left(\sqrt{S_1}d/2\right)}{\cos\left(\sqrt{S_2}d/2\right)} \cos\left(\sqrt{S_2}y\right) \right\}$$

$$+ \frac{k_+^2 - k_-^2}{4i\omega^2 \mu_c^2 \xi_c} S_1 F_2 \left\{ \sin\left(\sqrt{S_1}y\right) + \frac{\sin\left(\sqrt{S_1}d/2\right)}{\sin\left(\sqrt{S_2}d/2\right)} \sin\left(\sqrt{S_2}y\right) \right\}$$

$$\tag{6}$$

The transverse magnetic field components can be obtained from a knowledge of the transverse electric field components via the following relations

$$\begin{bmatrix} H_x \\ H_y \end{bmatrix} = \begin{pmatrix} -i\xi_c & \frac{-i\omega\varepsilon_c}{\gamma} \\ \frac{\gamma}{i\omega\varepsilon_c} & i\xi_c \end{pmatrix} \begin{bmatrix} E_x \\ E_y \end{bmatrix} \tag{7}$$

The dispersion relation for guided modes in this type of chirowave-break guides has also been analyzed [14,24]. It has the following form

$$\Delta \equiv \Delta_1 \cdot \Delta_2 = 0$$

with Δ_1 and Δ_2 defined as

$$\Delta_{\substack{1\\2}} = \left[\sqrt{1 - ((\beta + i\alpha)/k_+)^2} + \sqrt{1 - ((\beta + i\alpha)/k_-)^2} \right] \cdot$$

$$\sin\left(\frac{k_+ d\sqrt{1 - ((\beta + i\alpha)/k_+)^2} + k_- d\sqrt{1 - ((\beta + i\alpha)/k_-)^2}}{2} \right)$$

$$\pm \left[\sqrt{1 - ((\beta + i\alpha)/k_+)^2} - \sqrt{1 - ((\beta + i\alpha)/k_-)^2} \right] \cdot$$

$$\sin\left(\frac{k_+ d\sqrt{1 - ((\beta + i\alpha)/k_+)^2} - k_- d\sqrt{1 - ((\beta + i\alpha)/k_-)^2}}{2} \right)$$

$$\tag{8}$$

The above dispersion relation is valid for chirowaveguides filled with lossy, as well as lossless chiral materials. It presents the relations of α versus ω ($\omega - \alpha$ relation) and β versus ω ($\omega - \beta$ relation). These two relations can be plotted separately. Figure 2 presents these two plots for the case of parallel–plate chirowaveguide with parameters $\varepsilon_c = 2\varepsilon_0$, $\mu_c = \mu_0(1 + 0.5i)$ and $\xi_c = 0.001$ mho where ε_0 and μ_0 are permittivity and permeability of free space. Here μ_c is assumed to be

complex. [5] In this Figure, the normalized frequency Ω $\left(\equiv \omega d\sqrt{\mu_o \varepsilon_o}\right)$
is plotted versus normalized βd or normalized αd. Here even and
odd modes are denoted by (p) and (i), respectively. As described in
detail in [14, 24], some of the interesting features can be highlighted
here: first, we see from Fig. 2 that at $\omega = 0$, the values of $\beta = 0$
and $\alpha_{\text{cutoff}} = n\pi/d$ with $n = 0$, 1, 2, ... would make $\Delta_1 = 0$
and $\Delta_2 = 0$ simultaneously. However, as the frequency is increased,
the plot for $\Delta_1 = 0$ and the one for $\Delta_2 = 0$ would result in two
different sets of values for α and β. This is indeed the phenomenon
of *mode bifurcation* in lossy chirowaveguides, which for the lossless
chirowaveguides was originally studied in [13,14]. As discussed in detail
in [14,24], the guided modes corresponding to $\Delta_1 = 0$, for which F_1
in Eq. (5) is zero, are called even modes; and the ones resulting from
$\Delta_2 = 0$, for which $F_2 = 0$, are odd modes. For the lossless case,
it was shown that the plot of dispersion relation consists of a set of
bifurcated modes originating from common cut–off frequencies which
can be obtained by setting $\beta = 0$. This leads to $\Delta_1 = \Delta_2 = 0$ from
which the following expression for the cut–off frequencies for the loss-
less case is obtained:

$$\Omega_c \equiv \omega_c d\sqrt{\mu_c \varepsilon_c} = \frac{n\pi}{\sqrt{\frac{\mu_c}{\varepsilon_c}\xi_c^2 + 1}} \qquad \text{with } n = 0, 1, 2 \ldots \qquad (9)$$

---

[5] As we pointed out in [24], in this example the loss is phenomeno-
logically assumed to be represented as imaginary parts of complex per-
meablility $\mu_c = \mu_o(\mu' + i\mu'')$. In principle, all three material parame-
ters may be complex for lossy chiral materials [27,28]. However, here
to demonstrate the effect of loss in chiral materials and its underlying
physical insights on characteristics of guided modes in chirowaveguides
without introducing mathematical and numerical complexities of all–
complex parameters, we assume in this theoretical example that μ_c is
complex. The analysis given here can be easily expanded to the case
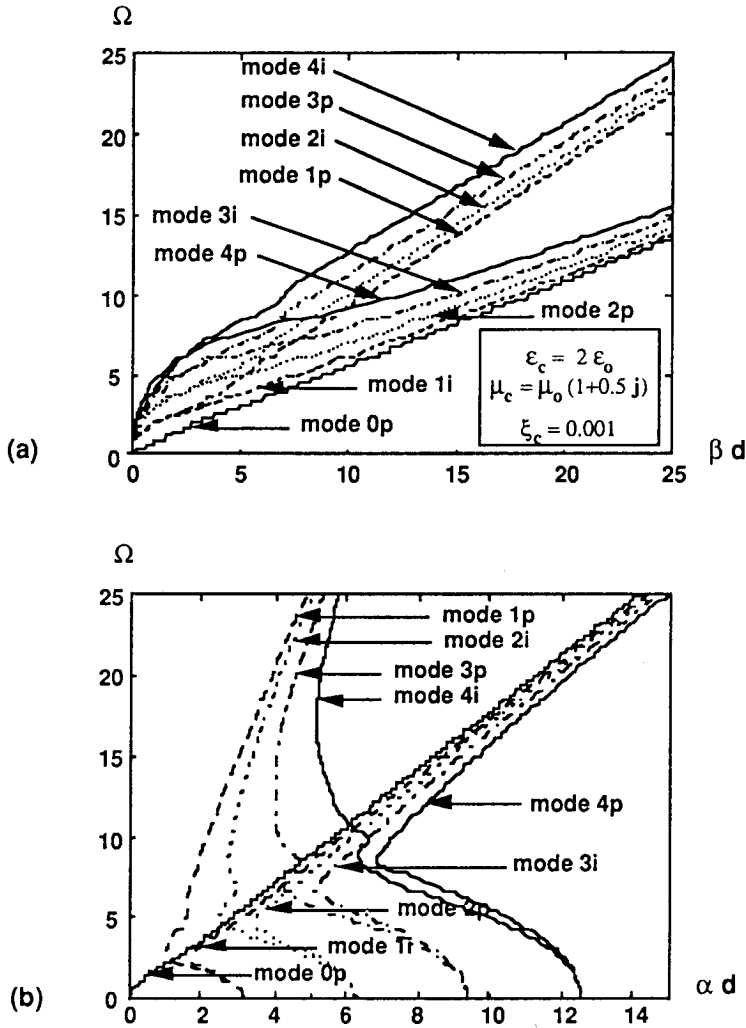of all three parameters being complex.

Figure 2a,b. The dispersion diagrams: (a) $\omega - \beta$ diagram and (b) $\omega - \alpha$ diagram for the parallel–plate metallic chirowaveguide in Fig. 1. The material parameters are taken to be $\epsilon_c = 2\epsilon_0, \mu_c = \mu_0(1 + 0.5i)$ and $\xi_c = 0.001$ mho. In (a) and (b), even and odd modes are denoted by (p) and (i), respectively.
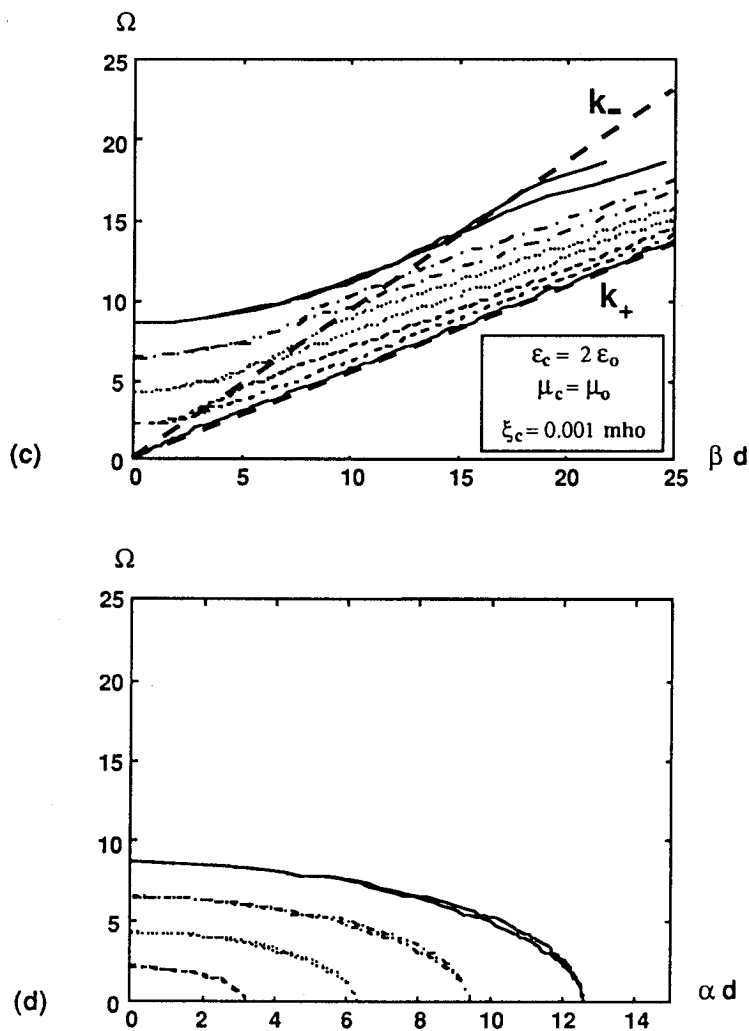
Figure 2c,d. The dispersion diagrams: Parts (c) and (d) are the $\omega - \beta$ and $\omega - \alpha$ diagrams for lossless material parameters $\epsilon_c = 2\epsilon_0, \mu_c = \mu_0$, and $\xi_c = 0.001$ mho.

We should mention that this mode bifurcation does not occur when $\xi_c = 0$, since for the nonchiral case, $\Delta_1 = \Delta_2 = 0$. The phenomenon of mode bifurcation was further studied in detail by Mahmoud [25]. He also pointed out that the dominant mode in the parallel–plate lossless chirowaveguide is an even mode and does not have any odd counterpart [25]. We also notice that for the lossy case, for large frequencies the values of β and α each approaches two different asymptotes. For the $\omega - \beta$ diagram, these asymptotes are indeed the linear function representing ω versus $\mathrm{Re}\,k_\pm$, and for the $\omega - \alpha$ diagram, this is the graph of ω versus $\mathrm{Im}\,k_\pm$. Therefore, in this case, we have two asymptotes in the $\omega - \beta$ diagram and two asymptotes in the $\omega - \alpha$ diagram. When $\xi_c = 0$, $k_\pm = k$ and we get one asymptote in each diagram. Furthermore, as the loss disappears, (i.e., $\mu'' \to 0$ in this example), the asymptotes in the $\omega - \alpha$ diagrams in Fig. 2 approaches the vertical axis, i.e., $\mathrm{Im}\,k_\pm \to 0$ Therefore the $\omega - \alpha$ diagram will then represent the evanescent modes in these waveguides. In the lossless case, the asymptote for the $\omega - \beta$ diagram is either k_+ or k_- depending on the sign of ξ_c [14,24]. In this limit, the starting points for dispersion curves in the $\omega - \beta$ diagrams in Figs. 2 will become the non–zero cutoff frequencies in the parallel–plate chirowaveguides. It is worth noting that in the non–chiral limit for the lossless case when $\xi_c = 0$, one of the modes of the bifurcated pair approaches conventional TM mode, whereas the other approaches the usual TE mode in the parallel–plate waveguide [14]. As is well known, in parallel–plate waveguides filled with non–chiral isotropic materials, the dispersion curves for TE modes overlap those of the TM modes. Therefore, the two curves of bifurcated pairs in the parallel–plate chirowaveguides become a single curve as ξ_c approaches zero. It appears that introduction of chirality in the material of these waveguides would have a tendency to bifurcate the set of otherwise degenerate modes. This theoretical observation is particularly supported by the fact that the dominant mode in these waveguides, which in the nonchiral case it is a TEM mode and unlike the higher–order modes it is not degenerate, would not become a bifurcated pair when the chirality in introduced in the material [25]. Figure 3 presents the sketch of the electric and magnetic field distribution in a parallel–plate chirowaveguide filled with chiral materials with parameters $\varepsilon_c = 2\varepsilon_0$, $\mu_c = \mu_0(1 + 0.5\mathrm{i})$ and $\xi_c = 0.001$ mho.

Ω

(e)

βd

$$\epsilon_c = 2\,\epsilon_o$$
$$\mu_c = \mu_o\,(1+0.5\,i)$$
$$\xi_c = 0$$
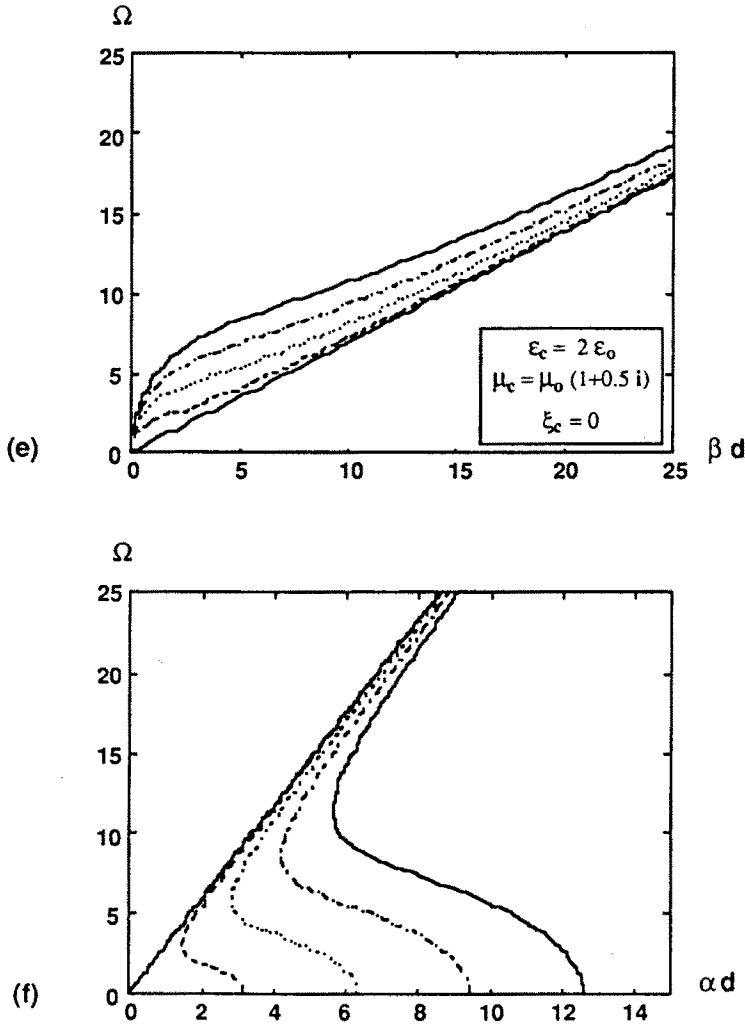
Ω

(f)

αd

Figure 2e,f.   The dispersion diagrams: For comparison, here are also shown the corresponding diagrams for the non–chiral cases: (e) and (f) present the $\omega - \beta$ and $\omega - \alpha$ diagrams for the lossy non-chiral case of $\epsilon_c = 2\epsilon_0, \mu_c = \mu_0(1 + 0.5i)$ and $\xi_c = 0$ mho; and (g) and (h) illustrate the diagrams for the lossless non-chiral case of $\epsilon_c = 2\epsilon_0, \mu_c = \mu_0$ and $\xi_c = 0$ mho.
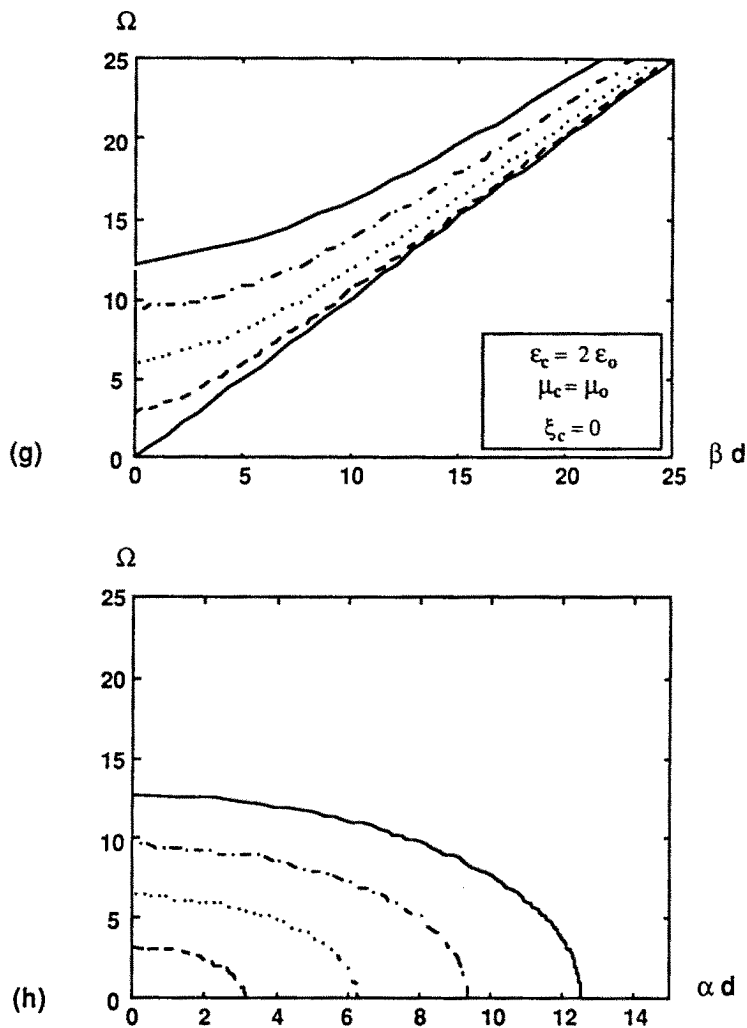
Figure 2g,h. The dispersion diagrams: (g) and (h) illustrate the diagrams for the lossless non-chiral case of $\epsilon_c = 2\epsilon_0, \mu_c = \mu_0$ and $\xi_c = 0$ mho.
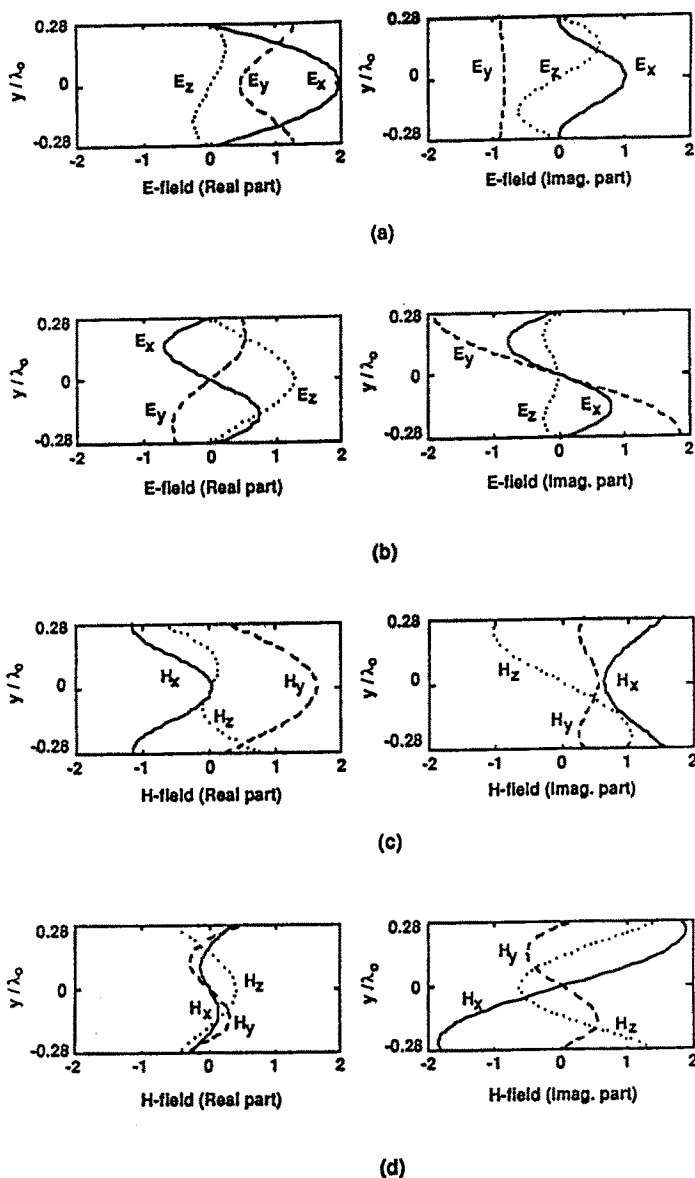
Figure 3. Sketch of (a)–(b) the electric field component, and (c)–(d) the magnetic field components across the cross section of the parallel–plate chirowaveguide (Fig. 1) as a function of y/λ_o where λ_o is the free space wavelength. There are two sets of plots for the electric field and magnetic field components : (a) and (c) field profiles of the odd mode of the first pair of bifurcated modes and (b) and (d) field profiles of even mode of the first bifurcated modes. The material parameters are $\epsilon_c = 2\epsilon_0, \mu_c = \mu_0(1 + 0.5i)$ and $\xi_c = 0.001$ mho.
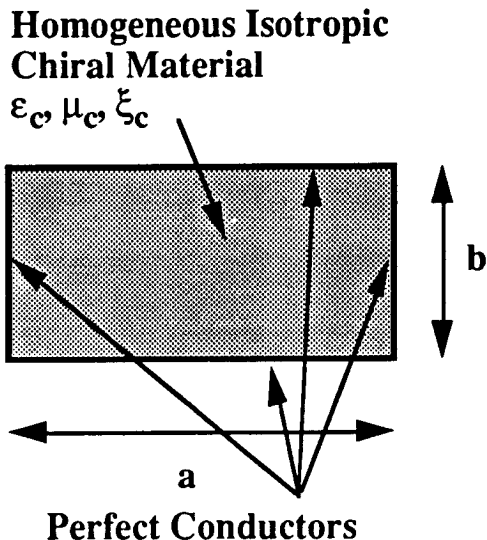
Homogeneous Isotropic
Chiral Material
$$\varepsilon_c, \mu_c, \xi_c$$

b

a

Perfect Conductors

Figure 4. Rectangular metallic chirowaveguide with dimensions a and b. The chiral material is assumed to be lossless.

4.   Metallic Rectangular Chirowaveguides

The problem of guided wave propagation in a rectangular waveguide with perfectly conducting walls and filled with lossless homogeneous chiral material has been studied recently in [29] where the finite–difference method (FDM) was used to solve the two coupled equations (4) for E_z and H_z. The dispersion diagrams were then obtained and plotted. Another approach to solve this problem was used by Cory [30] where he considered coupled differential equations for transverse variation of transverse field components and found a zero–order solution. Here we only review the highlights of the results in [29], such as dispersion characteristics of guided modes in such waveguides using the FDM. The reader may be referred to [29] for some detail of numerical analysis of this problem.

In applying the finite–difference method for this problem, a rectangular waveguide with dimensions $a = 2b$ filled with chiral material with parameters $\varepsilon_c = \varepsilon_o$, $\mu_c = \mu_o$ and $\xi_c = 0.001$ mho and 0.0005 mho is assumed (See Fig. 4). The dispersion diagrams are given in Figs. 5 and 6. As in the parallel–plate chirowaveguide, the cut–off frequencies
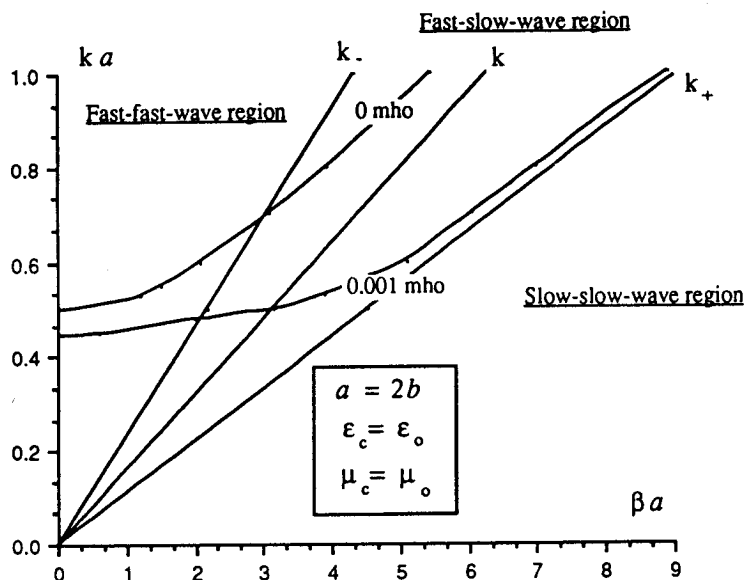
Figure 5. Dispersion diagram for the chirowaveguide in Fig. 4 with dimensions $a = 2b$. Here the non–chiral mode is TE_{10}. (From P. Pelet and N. Engheta, "Modal analysis of rectangular chirowaveguides with metallic walls using the finite–difference method," *J. Electromagnetic Waves and Applications*, Vol. 6, No. 9, 1277–1285, September 1992. Copyright @ 1992 VSP BV.)

are lower in the chiral ($\xi_c \neq 0$ mho) case than in the non–chiral case ($\xi_c = 0$ mho). Similar to the parallel–plate chirowaveguides, three regions in these diagrams can also be identified: the *fast–fast–wave* region for which the phase velocity v_p of the guided mode in the waveguide is greater than the phase velocities $v_+ = \omega/k_+$ and $v_- = \omega/k_-$ of the bulk eigenmodes, the *fast–slow–wave* region for which v_p is greater than v_+ but smaller than v_-, and the *slow–slow–wave* region for which v_p is greater than v_+ and v_-. Special attention must be paid to the mode bifurcation phenomenon. It can be seen that such bifurcation occurs for the modes which reduce to the non–chiral TE_{11} mode
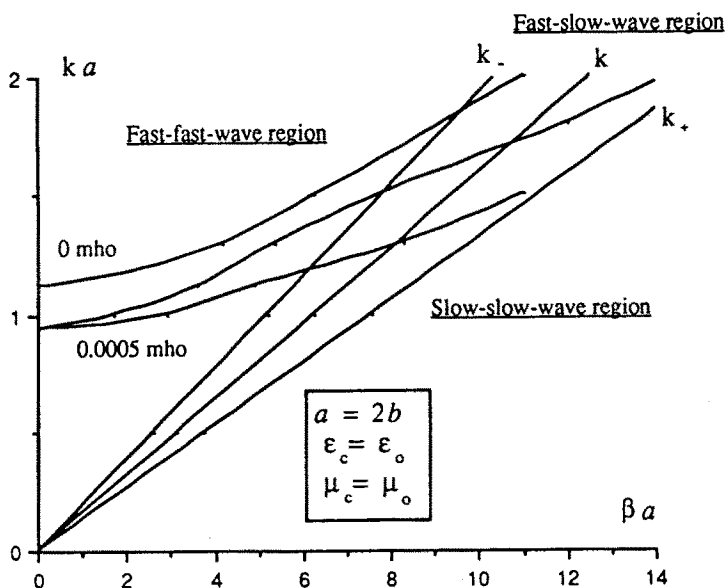
Figure 6. Dispersion diagram for the chirowaveguide in Fig. 4 with dimensions $a = 2b$. Here the non–chiral mode is TE_{11}. (From P. Pelet and N. Engheta, "Modal analysis of rectangular chirowaveguides with metallic walls using the finite–difference method," *J. Electromagnetic Waves and Applications*, Vol. 6, No. 9, 1277–1285, September 1992. Copyright © 1992 VSP BV.)

in the absence of chirality. However, bifurcation is not seen for the mode which approaches the non–chiral TE_{10} mode when $\xi_c = 0$ mho. This again supports the observation stated in the previous section. Since in the non–chiral case, the TE_{11} dispersion curve corresponds actually to both TM_{11} and TE_{11}, and since chirality will effectively influence TE and TM modes differently, the dispersion curves are going to split when $\xi_c \neq 0$ mho. However, the TE_{10} mode has no TM_{10} counterpart in the non–chiral case. As a result, in the chiral case the equivalent dispersion curve is not bifurcated.

5.   Metallic Circular Chirowaveguides: A Review

The case of circular cylindrical waveguide with perfectly conducting wall and filled completely with isotropic lossless chiral materials have been analyzed by Eftimiu and Pearson [15], Svedin [17], Mahmoud [25], and Hollinger *et al.* [19]. Rao has analyzed the attenuation properties of circular chirowaveguides when the attenuation is due to the lossy walls [31].

In these studies, electromagnetic properties of guided modes in such waveguides were studied, and relevant quantities such as dispersion relations, cutoff frequencies, field distributions, and polarization characteristics of guided modes were analyzed. It was found that due to the geometry of the problem, field quantities were expressed in terms of Bessel's functions as expected, and the two wave numbers $k_\pm$ played important roles. As in the case of the parallel–plate chirowaveguides, the cut off frequencies have been lowered by introduction of chirality in the medium. More importantly, the mode bifurcation was also observed for degenerate modes in such waveguides [17,25]. More specifically, since the waveguide's cross section is circular, in the non–chiral case any mode with any azimuthal dependence can have a degenerate counterpart mode whose fields are the same as the original mode but rotated $90°$ in the azimuth direction. For instance, in the non-chiral case, TE_{11} mode can have a degenerate counterpart, which is again TE_{11}, but its whole field distribution is rotated $90°$ around the z axis. [6] When the chirality is present in the material, such modes will become hybrid modes and they will have bifurcated dispersion curves in the dispersion diagram. However, if the mode in the non–chiral case is azimuthally symmetric, then in the chiral case, such a mode will again become hybrid but bifurcation phenomenon will not occur. For detailed description of electromagnetic characteristics of modes in circular metallic chirowaveguides, the reader is referred to [17,19].

Open dielectric circular chirowaveguides and the effect of chirality of the waveguide's material on guided modes have also been analyzed by Svedin [17].

---

[6]   More explicitly, if the azimuthal dependence of the first TE_{11} is $\sin\varphi$, the azimuthal dependence of the degenerate counterpart is $\cos\varphi$.

6.   Dielectric Slab Chirowaveguides

Open dielectric slab chirowaveguides are another canonical case of waveguiding structures with chiral materials. Owing to their possible applications in future devices and components, these guided-wave structures have been the subject of studies by several researchers, namely, Engheta and Pelet [26,36–37], Cory and Rosenhouse [32], Uslenghi and his co–workers [33–35], Oksanen et al. [38,39], Mahmoud [40] to name a few. The problem of chirowaveguides with impedance walls has been studied in detail by Mahmoud [41], and Oksanen et al. [42] .

The open single slab homogeneous chirowaveguides can be considered in two different cases: symmetric case where the chiral slab is surrounded by the same non–chiral medium in both sides; and the asymmetric case where the two surrounding media are different non–chiral materials (See Fig. 7). We have analyzed the first case, and the second case with a perfect conducting layer as one of the surrounding media [26]. The mathematical techniques used to solve the guided wave propagation in these chiral slabs are similar to those used for the metallic parallel–plate chirowaveguides. It was found that for the symmetric chiral slab of thickness d and material parameters ε_c, μ_c, ξ_c, surrounded by the free space with parameters ε_0 and μ_0, the dispersion relation for guided (bound) modes were $\Delta = \Delta_1 \cdot \Delta_2 = 0$, with

$$
\Delta_1 = \left[\frac{\omega\varepsilon_0 S_1}{\sqrt{S_0}} \sin\left(\sqrt{S_1}d/2\right) - \frac{k_+\sqrt{S_1}}{\eta_c} \cos\left(\sqrt{S_1}d/2\right) \right]
$$

$$
\times \left[k_-\sqrt{S_2} \cos\left(\sqrt{S_2}d/2\right) - \frac{\omega\mu_0 S_2}{\eta_c\sqrt{S_0}} \sin\left(\sqrt{S_2}d/2\right) \right]
$$

$$
+ \left[\frac{\omega\varepsilon_0 S_2}{\sqrt{S_0}} \sin\left(\sqrt{S_2}d/2\right) - \frac{k_-\sqrt{S_2}}{\eta_c} \cos\left(\sqrt{S_2}d/2\right) \right]
$$

$$
\times \left[k_+\sqrt{S_1} \cos\left(\sqrt{S_1}d/2\right) - \frac{\omega\mu_0 S_1}{\eta_c\sqrt{S_0}} \sin\left(\sqrt{S_1}d/2\right) \right] \quad (10a)
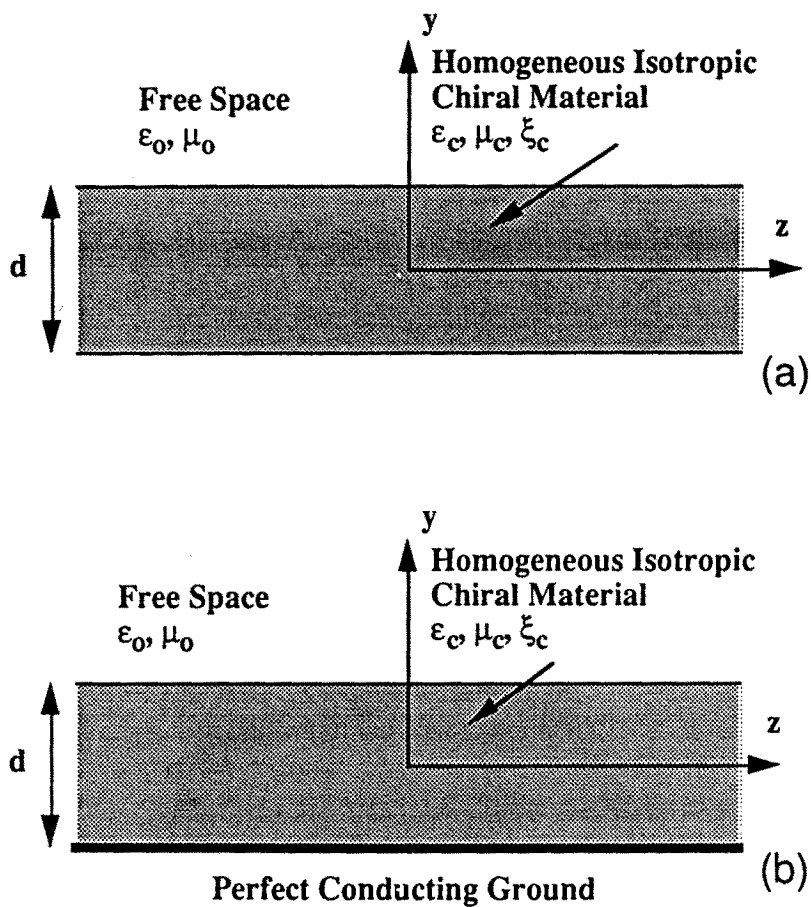$$

Figure 7. Symmetric (a) and grounded (b) lossless chiral slabs with material parameters ϵ_c, μ_c, and ξ_c.

$$\Delta_2 = \left[\frac{\omega\varepsilon_o S_1}{\sqrt{S_o}} \cos\left(\sqrt{S_1}d/2\right) + \frac{k_+\sqrt{S_1}}{\eta_c} \sin\left(\sqrt{S_1}d/2\right) \right]$$

$$\times \left[k_-\sqrt{S_2} \cos\left(\sqrt{S_2}d/2\right) + \frac{\omega\mu_o S_2}{\eta_c\sqrt{S_o}} \cos\left(\sqrt{S_2}d/2\right) \right]$$

$$+ \left[\frac{\omega\varepsilon_o S_2}{\sqrt{S_o}} \cos\left(\sqrt{S_2}d/2\right) + \frac{k_-\sqrt{S_2}}{\eta_c} \sin\left(\sqrt{S_2}d/2\right) \right]$$

$$\times \left[k_+\sqrt{S_1} \sin\left(\sqrt{S_1}d/2\right) + \frac{\omega\mu_o S_1}{\eta_c\sqrt{S_o}} \cos\left(\sqrt{S_1}d/2\right) \right] \quad (10b)$$

Here $S_o = \beta^2 - \omega^2\mu_o\varepsilon_o$, S_1 and S_2 have been defined earlier with $\gamma = i\beta$, [7] and η_c, k_+, k_- have all been specified before. The cutoff frequencies ω_c can then be obtained by setting $\beta = \omega_c\sqrt{\mu_o\varepsilon_o}$ in the above dispersion relation . Thus we get

$$\omega_c = \frac{m\pi}{\sqrt{\mu_o\varepsilon_o}\,d \left\{ \left(\pm\sqrt{\frac{\mu_c}{\varepsilon_c}}\xi_c + \sqrt{\frac{\mu_c}{\varepsilon_c}\xi_c^2 + 1} \right)^2 \frac{\mu_c\varepsilon_c}{\mu_o\varepsilon_o} - 1 \right\}^{0.5}} \quad (11)$$

for $m = 0, 1, 2, \ldots$. The electric field expressions for the inside and outside the chiral slab have also been obtained [26]. For the inside the slab where $-(d/2) \leq y \leq d/2$, we have

$$E_{ox}^e = \pm k_+\sqrt{S_1} \left[\begin{matrix} \cos \\ \sin \end{matrix} \left(\sqrt{S_1}y\right) - \Gamma_o^e \frac{k_-}{k_+} \begin{matrix} \cos \\ \sin \end{matrix} \left(\sqrt{S_2}y\right) \right] e^{i\beta z} \quad (12a)$$

$$E_{oy}^e = \pm i\beta\sqrt{S_1} \left[\begin{matrix} \cos \\ \sin \end{matrix} \left(\sqrt{S_1}y\right) + \Gamma_o^e \begin{matrix} \cos \\ \sin \end{matrix} \left(\sqrt{S_2}y\right) \right] e^{i\beta z} \quad (12b)$$

$$E_{oz}^e = S_1 \left[\begin{matrix} \sin \\ \cos \end{matrix} \left(\sqrt{S_1}y\right) + \Gamma_o^e \frac{\sqrt{S_2}}{\sqrt{S_1}} \begin{matrix} \sin \\ \cos \end{matrix} \left(\sqrt{S_2}y\right) \right] e^{i\beta z} \quad (12c)$$

---

[7] Here, the materials are taken to be lossless and the modes under consideration are assumed to be guided (bound). Therefore, the wavenumbers of such modes are expressed as $\gamma = i\beta$, and the attenuation rate $\alpha = 0$.

where

$$\Gamma_{\substack{e\\o}} \equiv \frac{\omega\mu_o\sqrt{S_1}\frac{\sin}{\cos}\left(\sqrt{S_1}d/2\right) \mp \eta_c\sqrt{S_o}k_+\frac{\cos}{\sin}\left(\sqrt{S_1}d/2\right)}{\omega\mu_o\sqrt{S_2}\frac{\sin}{\cos}\left(\sqrt{S_2}d/2\right) \mp \eta_c\sqrt{S_o}k_-\frac{\cos}{\sin}\left(\sqrt{S_2}d/2\right)}$$

and for the region above the chiral slab, i.e., $d/2 \leq y$, we get

$$E_{\substack{e\\o}x} = \pm k_+\sqrt{S_1}$$

$$\cdot \left[\frac{\cos}{\sin}\left(\sqrt{S_1}d/2\right) - \Gamma_{\substack{e\\o}}\frac{k_-}{k_+}\frac{\cos}{\sin}\left(\sqrt{S_2}d/2\right)\right]e^{-\sqrt{S_o}(y-d/2)}e^{i\beta z} \quad (13a)$$

$$E_{\substack{e\\o}y} = \pm i\beta\frac{\varepsilon_c}{\varepsilon_o}\sqrt{S_1}$$

$$\cdot \left[\frac{\cos}{\sin}\left(\sqrt{S_1}d/2\right) + \Gamma_{\substack{e\\o}}\frac{\cos}{\sin}\left(\sqrt{S_2}d/2\right)\right]e^{-\sqrt{S_o}(y-d/2)}e^{i\beta z} \quad (13b)$$

$$E_{\substack{e\\o}z} = S_1\left[\frac{\sin}{\cos}\left(\sqrt{S_1}d/2\right) + \Gamma_{\substack{e\\o}}\frac{\sqrt{S_2}}{\sqrt{S_1}}\frac{\sin}{\cos}\left(\sqrt{S_2}d/2\right)\right]$$

$$\cdot e^{-\sqrt{S_o}(y-d/2)}e^{i\beta z} \quad (13c)$$

For the region below the slab where $y \leq d/2$, the electric field expressions can be written straightforwardly using the symmetry. The magnetic field can also be obtained from the above field expressions using the Maxwell equations.

The dispersion diagram of the symmetric slab chirowaveguide is shown in Fig. 8. This plot is for material parameters $\varepsilon_c = 2\varepsilon_o, \mu_c = \mu_o$, and $\xi_c = 0.0005$ mho. Figure 9 also presents plots of normalized field intensities of electric field components of lowest odd guided mode in the dielectric slab chirowaveguide. It can be easily shown that the cutoff frequencies and the field expressions approach those of the non–chiral slab waveguides when $\xi_c \to 0$. In this limit, $\Delta_1 = 0$ provides the dispersion relation for odd TE and TM modes of the non–chiral slabs, whereas $\Delta_2 = 0$ gives up the dispersion relation for even TE and TM modes [43]. So we note that for the non–chiral case, TE and TM modes of the same order and the same parity (odd or even) share the same cutoff frequencies. However, when the chirality is introduced, i.e., $\xi_c \neq 0$, then as can be seen from Eq. (11) for modes with $n \neq 0$ the cutoff frequencies would split. Such splitting of cutoff frequencies for $n \neq 0$ modes can be observed in Fig. 8.

The grounded asymmetric slab chirowaveguides have also been analyzed using similar analyses. The results for the dispersion relations and field expressions can be obtained in [26,37].
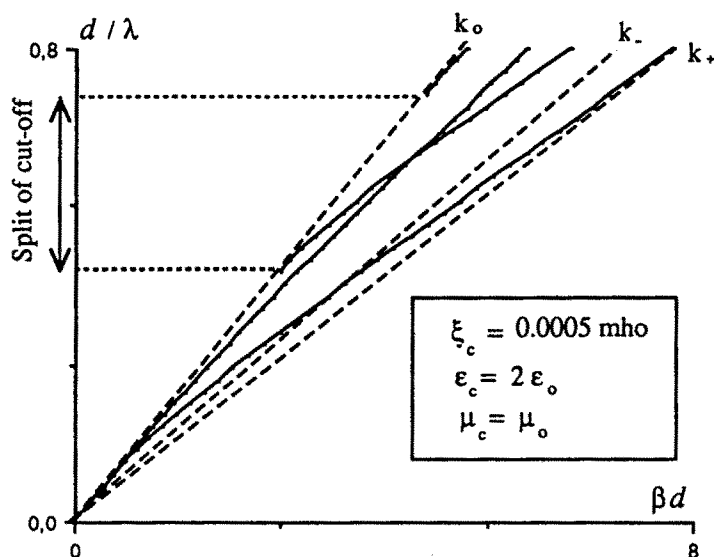
Figure 8. Dispersion diagram of symmetric chiral slab in Fig. 7(a). (From N. Engheta and P. Pelet, "Surface waves in chiral layers," *Optics Letters,* Vol. 16, No. 10, 723–725, May 15, 1991. Copyright @ 1991, Optical Society of America)

7. Mode Orthogonality and Mode Coupling in Chirowaveguides

As in conventional non–chiral cylindrical waveguides, modes in cylindrical chirowaveguides satisfy certain orthogonality relations. Such relations have been studied and reported in the literature [44]. It has been shown that in lossless chirowaveguides with arbitrary cross sectional shape, the following orthogonality relation can be written

$$\iint\limits_{S} (e_m \times h_n^* + e_n^* \times h_m) \cdot \hat{z}\, dS = 4P_n Sgn(n)\delta_{mn} \qquad (14)$$
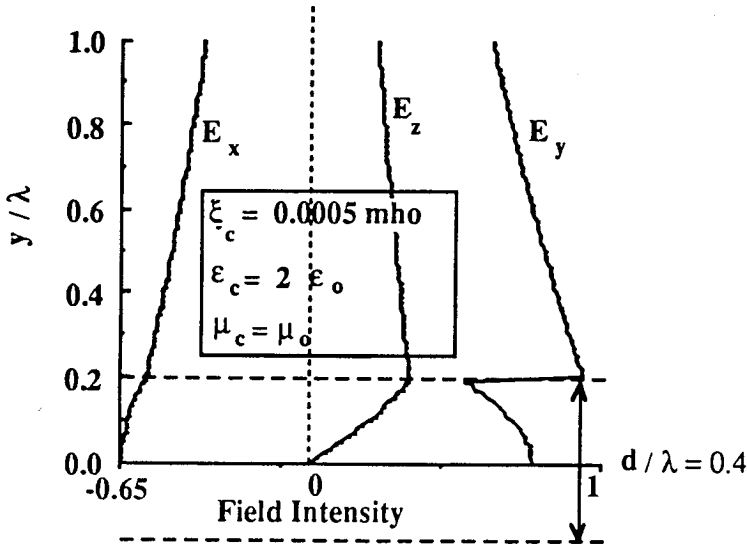
Figure 9. Sketch of normalized electric field intensities in the symmetric chiral slab in Fig. 7(a). The material parameters are $\epsilon_c = 2\epsilon_0, \mu_c = \mu_0$ and $\xi_c = 0.0005$ mho. (From N. Engheta and P. Pelet, "Surface waves in chiral layers," *Optics Letters,* Vol. 16, No. 10, 723–725, May 15, 1991. Copyright @ 1991, Optical Society of America)

where $\mathbf{e}_m, \mathbf{h}_m, \mathbf{e}_n$, and $\mathbf{h}_n$ are parts of mth and nth guided modes in the guide, i.e., $\mathbf{E}_m = \mathbf{e}_m \exp(i\beta_m z), \mathbf{H}_m = \mathbf{h}_m \exp(i\beta_m z), \mathbf{E}_n = \mathbf{e}_n \exp(i\beta_n z)$, and $\mathbf{H}_n = \mathbf{h}_n \exp(i\beta_n z)$, $\hat{z}$ is the unit vector along the waveguide's axis, P_n is the power carried by the nth mode, δ_{mn} is a Kronecker delta, and $*$ is the complex conjugation. The surface integral is carried out over the transverse plane of the waveguide [44]. Another form of orthogonality relation, which is valid for lossy as well as lossless chirowaveguides, has been studied, and it is given [44] as

$$\iint\limits_{S} (\mathbf{e}_m \times \mathbf{h}_n - \mathbf{e}_n \times \mathbf{h}_m) \cdot \hat{z}\, dS = 0 \qquad (15)$$

The above orthogonality relations are similar to those given for gyrotropic waveguides [45].

These orthogonality relations enable one to obtain expressions for mode coupling in chirowaveguides due to perturbation. As was shown in Eq. (4), the chirality of medium would result in coupling of longitudinal components of electric and magnetic fields in such waveguides. Without chirality in simple non–chiral metallic cylindrical waveguides these two components are decoupled. When chirality is introduced these components, and their corresponding transverse components, are coupled. Therefore, one can regard such mode coupling as coupling of modes due to chirality as perturbation in an otherwise non–chiral waveguide [46]. As can be shown in [46], these "perturbed" modes can be expressed in terms of "unperturbed" modes, i.e. modes in non–chiral waveguides, i.e.,

$$\mathbf{E}' \approx \sum_m a_m(z)\mathbf{e}_m\,e^{i\beta_m z} \tag{16}$$

$$\mathbf{H}' \approx \sum_m a_m(z)\mathbf{h}_m\,e^{i\beta_m z} \tag{17}$$

where $\mathbf{e}_m\,e^{i\beta_m z}$ and $\mathbf{h}_m\,e^{i\beta_m z}$ are normalized unperturbed modes (with $\mathbf{e}_m$ and $\mathbf{h}_m$ depend only on the transverse coordinates), and $a_m(z)$ are expansion coefficients, which in general vary with z. Following standard techniques in deriving the coupled–mode equation, one can get the following coupled equations for coefficients $a_m(z)$:

$$\frac{da_n(z)}{dz} = \sum_m a_m(z)e^{i(\beta_m - \beta_n)z}C_{mn} \tag{18}$$

where C_{mn} is the coupling coefficient defined as

$$C_{mn} \equiv \frac{1}{4Sgn(n)} \iint\limits_S \omega\mu_c\xi_c\left(\mathbf{e}_m\cdot\mathbf{h}_n^* - \mathbf{e}_n^*\cdot\mathbf{h}_m\right)\,dS \tag{19}$$

As can be seen the coupling coefficients C_{mn} are directly proportional with chirality admittance ξ_c. When $\xi_c = 0$, then unperturbed modes are decoupled as expected.

The coupling of modes in and among waveguides filled with chiral materials have been studied by several researchers, namely, Chan and Uslenghi [34,47,48], Mazur *et al.* [49], Cory and Rosenhouse [50–52], Chein *et al.* [53], etc. In their analyses, they have shown interesting properties of mode coupling in such waveguides, and they have proposed some novel applications for coupling of modes in these guided–wave structures.

8.   Partially Filled Chirowaveguides: A Review

In the metallic chirowaveguides reviewed so far, the guiding regions have been completely filled with chiral materials. In the case of open chirowaveguides, the regions where guided modes are mostly confined are also made of chiral materials completely. However, the cases of waveguides wherein the guiding regions are *partially* filled with these materials are of equal importance. This is mainly due to the fact that in such structures, there are more parameters involved, e.g., sizes of the chiral and non–chiral regions, which can affect propagation characteristics of guided modes.

The waveguides partially filled with chiral material can be categorized into two general cases: partially filled chirowaveguides wherein the chiral materials are placed longitudinally along the waveguides' axes; and those within which chiral materials are transversely located. [8] In the first case, since the materials are placed along the waveguide's axis (i.e., the structure is homogeneous in the z direction, but not in the transverse directions), electromagnetic properties of guided modes are independent of the z coordinate (of course, with the exception of propagator $\exp(i\beta z)$). As a result, modes will not be reflected. However, if the material is transversely located, i.e., the homogeneity is along the transverse directions, guided modes can be reflected and transmitted due to inhomogeneity along the z direction.

The various forms of partially–filled chirowaveguides of first kind have been analyzed by several researchers. Among these one can mention Toscano *et al.* [54,55] who analyzed the dispersion characteristics of guided modes in parallel–plate waveguides which are partially and longitudinally filled with chiral material, Monte and Uslenghi [35] who studied the modes in circular cylindrical dielectric–chiral cables, Mahmoud [56] with his analysis of circular chirowaveguides with dielectric linings, Saadoun [57] with work on the effect of a chiral rod in waveguide with arbitrary cross section, and Tretyakov and Viitanen [58] who considered perturbation techniques in cavity resonators and waveguides due to a biisotropic inclusions.

---

[8]   Of course, one can also assume that the chiral material is inhomogeneous in both the transverse and longitudinal directions. Here, we restrict ourselves to the cases where the material homogeneity is either in the transverse or in the longitudinal directions.
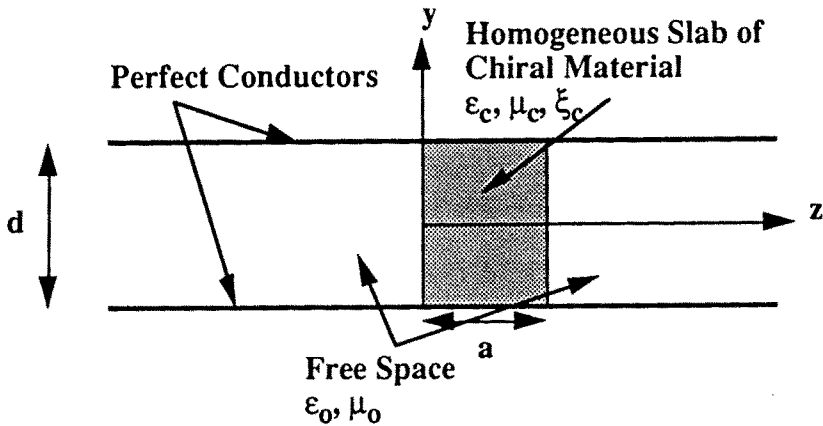
Figure 10. A slab of chiral material transversely located in a parallel–plate waveguide. The electromagnetic quantities here are independent of x direction.

The second kind of partially filled chirowaveguides, i.e., transversely located chiral materials in a chirowaveguide has also been analyzed for some cases. Rong studied circular chirowaveguides periodically loaded with metal grating [59]. Mariotte and Engheta studied the reflection and transmission of guided modes at a dielectric–chiral interface and at a chiral slab in a parallel–plate chirowaveguide [60,61]. For the slab case, the lossy chiral material was also considered [61]. They considered a chiral slab of thickness a located transversely in a parallel–plate waveguide. The slab is placed between the plane $z = 0$ and $z = d$ as shown in Fig. 10. The incident wave is assumed to be a TEM mode, incident from the region $z < 0$, and polarized with the electric field intensity E_o along the y direction. The reflected and transmitted waves outside the slab region can be expressed as a sum of the modes in the parallel–plate waveguide, and the wave inside the slab can also be expanded in terms of all the positive-z-going and negative-z-going hybrid modes in parallel–plate chirowaveguides. Since the modes in the chiral slab (both propagating and evanescent)
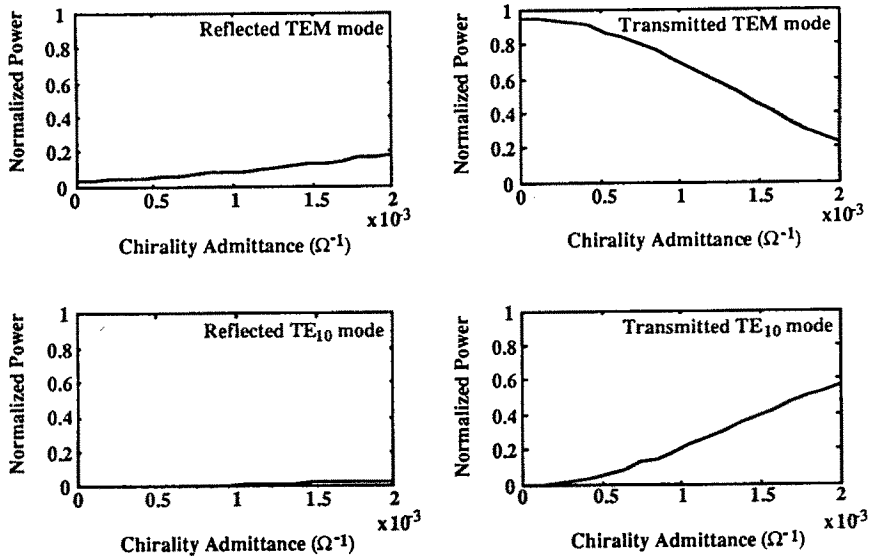
Figure 11. Normalized power of TEM and TE_{10} modes in the reflection and transmission waves for geometry of Fig. 10. Here $d/\lambda_0 = 0.56, a/d = 0.5$, and $\epsilon_c = 2\epsilon_0$ and $\mu_c = \mu_0$. Normalization is with respect to the power (per unit length in the x direction) of the incident TEM mode. (From F. Mariotte and N. Engheta, "Reflection and transmission of guided electromagnetic waves at an air–chiral interface and at a chiral slab in a parallel–plate waveguide," *IEEE Trans. Microwave Theory and Techniques*, Vol. MTT–41, No. 11, 1895–1906, November 1993. Copyright @ 1993, IEEE).

are hybrid, the boundary conditions for the electric and magnetic field components require that higher order modes of TE and TM be considered in the air region ($z < 0$ and $z > a$) in addition to the dominant TEM mode. Of course, some (or sometime all) of these higher order modes are evanescent and the rest are propagating. Following these steps and satisfying boundary conditions at the two air–chiral inter-
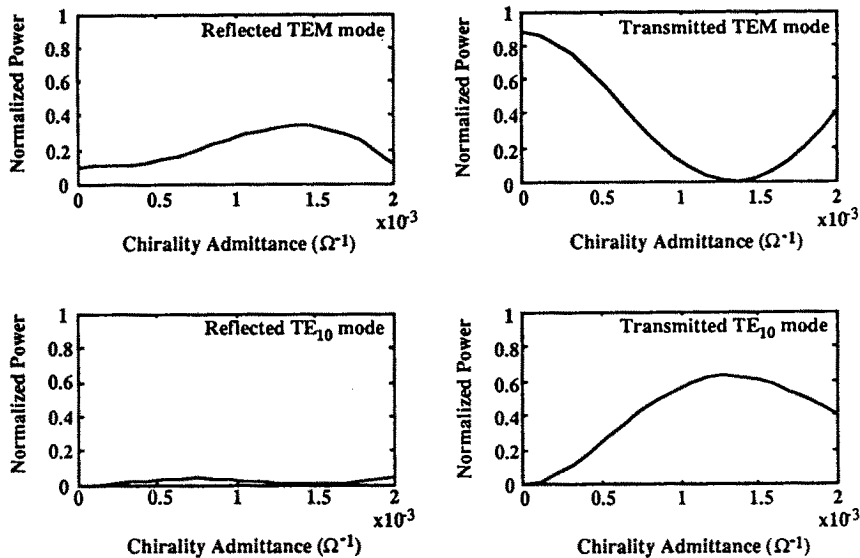
Figure 12. Normalized power of TEM and TE$_{10}$ modes in the reflection and transmission waves for geometry of Fig. 10. Here $d/\lambda_0 = 0.56, a/d = 1$, and $\epsilon_c = 2\epsilon_0$ and $\mu_c = \mu_0$. Normalization is with respect to the power (per unit length in the x direction) of the incident TEM mode. (From F. Mariotte and N. Engheta, "Reflection and transmission of guided electromagnetic waves at an air–chiral interface and at a chiral slab in a parallel–plate waveguide," *IEEE Trans. Microwave Theory and Techniques*, Vol. MTT–41, No. 11, 1895–1906, November 1993. Copyright @ 1993, IEEE).

faces (i.e., $z = 0$ and $z = a$), the relations between the reflected and transmitted waves with the incident TEM mode are analyzed [60]. The detailed analysis can be found in [60]. Figures 11 and 12 show the normalized power carried by the reflected and transmitted modes as a function of chirality for a chiral slab with thickness $a/d = 0.5$ and 1, respectively. The other material parameters of the chiral slab

are taken to be $\varepsilon_c = 2\varepsilon_0$ and $\mu_c = \mu_0$, and the waveguide thickness is $d/\lambda_0 = 0.56$, where λ_0 is the free space wavelength. For this value of d/λ_0, the parallel–plate waveguide can operate above the first non–zero cutoff frequency, and therefore in addition to the dominant TEM mode, the next higher order mode, i.e., TE_{10} can also propagate. Owing to the chirality of the slab, the modes in the slab are hybrid, and as a result TE_{10} mode can be excited. That is why in Figs. 11 and 12, the reflected and transmitted power are represented for TEM and TE_{10} modes separately. When chirality goes to zero, TE_{10} modes vanish, and only TEM modes contribute to reflected and transmitted power. One can also note that for the transmitted power in the region $z > a$ is virtually switched from TEM to TE_{10} and back, as the slab thickness a/d increases or chirality ξ_c increases. This is mainly due to the fact that the polarization of the transverse portion of electric field effectively "rotates" as the wave traverses the chiral slab, and therefore when the wave exits from the slab the relative values of E_x and E_y at $z = a$ plays an important role in exciting transmitted TEM and TE_{10} modes. Needless to say, the geometry of the waveguide, i.e., dimension d has also affected such rotation and contribution to these modes. This characteristics can have possible applications for design of novel devices such as $TE \leftrightarrow TM$ converters and polarization filters. As mentioned in [60], we should notice that here in the case of chiral slab inserted in the parallel–plate waveguide, the reflected wave can possess a cross polarization for its electric field in the transverse plane. This is primarily due to the effect of bounded structures (or waveguide's walls) which were not present for the unbounded case. In the unbounded situation where there is no waveguide, and there is a two dimensional chiral slab with thickness a illuminated with a normal incident linearly polarized wave, the reflected wave does not contain any cross polarization for its electric field. The transmitted wave is of course linearly polarized with a plane of polarization rotated by an angle $\varphi = \omega\mu_c\xi_c a$ [62]. This effect in chiral slab inserted in parallel–plate chirowaveguides may potentially be exploited for measuring the chiral properties of the slab using reflection properties.

When the loss is introduced in the chiral slab as an imaginary part of complex ε_c or complex μ_c, the reflection and transmission properties of these guided modes in the parallel–plate waveguide are affected [61]. Figure 13 presents the normalized absorbed power as a function of chirality admittance for the chiral slab of thickness $a/d =$
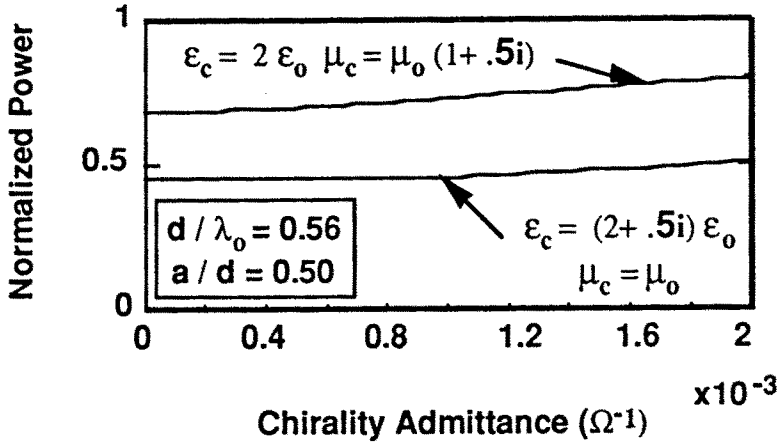
Figure 13. Normalized absorbed power in the slab shown in Fig. 10 as a function of ξ_c. Here $d/\lambda_0 = 0.56, a/d = 0.5$, and $\epsilon_c = 2\epsilon_0$ and $\mu_c = \mu_0(1+0.5i)$ for one curve and $\epsilon_c = (2+0.5i)\epsilon_0$ and $\mu_c = \mu_0$ for the other curve. Normalization is with respect to the power (per unit length in the x direction) of the incident TEM mode.

0.5 inserted transversely in a parallel–plate waveguide of thickness $d/\lambda_o = 0.56$. The other material parameters of the slab is $\varepsilon_c = 2\varepsilon_o$ and $\mu_c = \mu_o(1+0.5i)$ for one of the curves and $\varepsilon_c = (2+0.5i)\varepsilon_o$ and $\mu_c = \mu_o$ for the other curve.

9.   Potential Applications

Some of the interesting features and characteristics of guided modes in chirowaveguides could be a basis for novel and interesting potential applications in optics, microwave and millimeter wave regimes. These potential applications include conceptual ideas for some novel mode converters and directional couplers and switches [13,46–48,51] and distributed coupling via chirality [49], idea of chiral layers as antenna substrates and superstrates [36,37,63], possible applications to

phase shifter [57], etc. Guided–wave structures with chiral materials can also be used to measure chiral material parameters. This technique has been used by Hollinger *et al.* [64] to experimentally characterize microwave chiral composites in circular waveguides, and results of rotary dispersion and axial ratio of chiral samples have been reported. The analysis of reflection and transmission properties of a chiral slab inserted in parallel–plate waveguides should be expanded to include the inverse problem, namely, to express the material parameters in terms of reflection and transmission coefficients from chiral slabs in parallel–plate waveguides. Care must be taken in addressing the uniqueness of the results. In that case, the chirowaveguides can potentially be used to obtain material parameters in terms of reflection and transmission information.

10.   Summary

In this chapter, we briefly review certain electromagnetic characteristics and features of guided modes in cylindrical waveguides containing isotropic chiral materials. Basic formulation for guided mode propagation in chirowaveguides were reviewed and the cases of parallel–plate metallic chirowaveguide, metallic rectangular and circular chirowaveguides, open dielectric chirowaveguides were mentioned. Mode coupling in such guided–wave structures was also reviewed. Furthermore, partially filled chirowaveguides were also addressed and reviewed. It must be noted that, in addition to waveguiding properties of chiral materials, the electromagnetic characteristics of guided modes in bi-isotropic (materials with four parameters) and bi–anisotropic media have also been studied extensively in recent years. The reader is referred to the work of Uslenghi and co–workers [65,66], Paiva and Barbosa [67,68], Tretyakov and Viiatanen [58], Viitanen and Lindell [69], and Mazur [70] to name a few.

References

1. Lakhtakia, A., V. V. Varadan, and V. K. Varadan, *Time-Harmonic Electromagnetic Fields in Chiral Media,* Springer-Verlag, Berlin, 1989.

2. Jaggard, D. L., and N. Engheta, "Chirality in electrodynamics: modeling and applications" a chapter in *Directions in Electromagnetic Wave Modelling,* Editors H. L. Bertoni, and L. B. Felsen, Plenum Publishing Corporation, 485–493 1991.

3. Lakhtakia, A., (ed.), *Selected papers on Natural Optical Activity,* SPIE Opt. Eng. Press, Bellingham, WA, 1990.

4. Engheta, N., (guest ed.), Special issue of *Journal of Electromagnetic Waves and Applications on Wave Interactions with Chiral and Complex Media,* Vol. 6, No. 5/6, May–June 1992.

5. Kong, J. A., "Theorems of bianisotropic media," *Proc. IEEE,* Vol. 60, 1036–1046 (1972). See also J. A. Kong, *Electromagnetic Wave Theory,* Wiley Interscience, New York, 1986.

6. Post, E. J., *Formal Structure of Electromagnetics,* Amsterdam, North-Holland, 1962.

7. Bohren, C. F., "Scattering of electromagnetic waves by an optically active cylinder," *J. Colloid Interface Sci.,* Vol. 66, 105–109, Aug. 1978.

8. Jaggard, D. L., A. R. Mickelson, and C. H. Papas, "On electromagnetic waves in chiral media," *J. Applied Physics,* Vol. 28, 211–216, 1979.

9. Bassiri, S., N. Engheta and C. H. Papas, "Dyadic Green's Function and Dipole Radiation in Chiral Media," *Alta Frequenza,* LV-2, 83–88, 1986.

10. Sihvola, A. H., and I. V. Lindell, "Biisotropic constitutive relations," *Microwave and Opt. Tech. Lett.,* Vol. 4, No. 7, 1991.

11. Silverman, M. P., "Reflection and refraction at the surface of a chiral medium: comparison of gyrotropic constitutive equations," *Lett. Nuovo Cimento,* Vol. 43, 378–382, 1985.

12. Lakhtakia, A., V. V. Varadan, and V. K. Varadan, "Field equations, Huygens's principle, integral equations, and theorems for radiation and scattering of electromagnetic waves in isotropic chiral media," *J. Opt. Soc. Am.* A Vol. 5, No. 2, 175–183, 1988.

13. Engheta, N., and P. Pelet, "Modes in chirowaveguides," *Optics Lett.,* Vol. 14, No. 11, 593–595, June 1989.

14. Pelet, P., and N. Engheta, "The theory of chirowaveguides," *IEEE Trans. Antennas and Propagat.*, Vol. AP–38, No. 1, 90–98, January 1990.

15. Eftimiu, C., and L. W. Pearson, "Guided electromagnetic waves in chiral media," *Radio Science*, Vol. 24, 351–359, 1989.

16. Varadan, V. K., A. Lakhtakia, and V. V. Varadan, "Propagation in a parallel plate waveguide wholly filled with a chiral medium," *J. Wave–Material Interaction*, Vol. 3, 267–272, 1988.

17. Svedin, J. A. M., "Propagation analysis of chirowaveguides using the Finite–Element Method," *IEEE Trans. Microwave Theory and Techniques*, Vol. 38, No. 10, 1488–1496, 1990.

18. Svedin, J. A. M., "Finite–element analysis of chirowaveguides," *Electronics Letters*, Vol. 26, No. 13, 928–929, 1990.

19. Hollinger, R. D., V. V. Varadan, and V. K. Varadan, "Eigenmodes in a circular waveguide containing an isotropic chiral material," *Radio Science*, Vol. 26, No. 5, 1335–1344, September–October 1991.

20. Collin, R. E., *Field Theory of Guided Waves*, McGraw–Hill Book Company, New York, 1960.

21. Yeh, C., "The elliptical dielectric waveguides," *J. Appl. Phys.*, Vol. 33, p. 3235, 1962.

22. Kales, M. L, "Modes in wave guides containing ferrites," *J. of Applied Physics*, Vol. 24, No. 5, 604–608, 1953.

23. Hlawiczka, P., *Gyrotropic Waveguides*, Academic Press, New York, 1981.

24. Mariotte, V., and N. Engheta, "Effect of chiral material loss on guided electromagnetic modes in parallel–plate chirowaveguides," *J. of Electromagnetic Waves and Applications*, Vol. 7, No. 10, 1307–1321, October 1993.

25. Mahmoud, S. F., "On mode bifurcation in chirowaveguides with perfect electric walls," *J. Electromagnetic Waves and Applications*, Vol. 6, No. 10, 1381–1392, 1992.

26. Engheta, N., and P. Pelet, "Surface waves in chiral layers," *Optics Letters*, Vol. 16, No. 10, 723–725, May 15, 1991.

27. Karlsson, A., and G. Kristensson, "Constitutive relations, dissipation, and reciprocity for the Maxwell equations in the time domain," *J. Electromagnetic Waves and Applications*, Vol. 6, No. 5/6, 537–552, May–June 1992.

28. Umari, M. H., V. V. Varadan, and V. K. Varadan, "Rotation and dichroism associated with chiral composite samples," *Radio Science*, Vol. 26, 1327–1334, 1991.

29. Pelet, P., and N. Engheta, "Modal analysis of rectangular chirowaveguides with metallic walls using the finite-difference method," *J. of Electromagnetic Waves and Applications, Special Issue on Materials and Measurement Techniques*, Vol. 6, No. 9, 1277–1285, September 1992. (Note a minor typographircal misprint on page 1280, third line after Eq. (6) where $H_z = 0$ should read $\frac{\partial H_z}{\partial n} = 0$.

30. Cory, H., "Wave propagation along a closed rectangular chirowaveguide," *Microwave and Optical Technology Letters*, Vol. 6, No. 14, 797–800, 1993.

31. Rao, T. C., "Attenuation characteristics of a circular chirowaveguide," *Electronics Letters*, Vol. 26, No. 21, 1767–1769, 1990.

32. Cory, H., and I. Rosenhouse, "Electromagnetic wave propagation along a chiral slab," *IEE Proc. Pt. –H, Microwave, Antennas, Propagation*, Vol. 138, No. 1, 51–54, 1991.

33. Ali, J. D., and P. L. E. Uslenghi, "Propagation in certain magnetoelectric slab Waveguides," Abstract in the *Digest of the 1992 National Radio Science Meeting*, Boulder, Colorado, p. 8, January 7–10, 1992.

34. Chan, K.-S., and P. L. E. Uslenghi, "Theory of chiral rectangular waveguide in dielectric substrate," Abstract in *Proc. of Progress in Electromagnetics Research Symposium*, (PIER 91), Cambridge, Massachusetts, July 1–5, p. 338, 1991.

35. Monte, T. D., and P. L. E. Uslenghi, "Modal theory for a chiral–dielectric cable," Abstract in *Proc. of the 1990 IEEE AP–S International Symposium/Radio Science Meeting*, Vol. Radio Science Meeting, Dallas, Texas, p. 135, May 7–11, 1990.

36. Engheta, N., and P. Pelet, "Reduction of surface waves in chirostrip antennas," *Electronics Letters*, Vol. 27, No. 1, 5–7, January 3, 1991.

37. Pelet, P., and N. Engheta, "Chirostrip antennas: line source problem," *J. Electromagnetic Waves and Applications*, Vol. 6, No. 5/6, 771–793, May–June 1992.

38. Oksanen, M. I., P. K. Koivisto, and I. V. Lindell, "Dispersion curves and fields for a chiral slab waveguides," *IEE Proc. Pt- H.,* Vol. 138, No. 4, 327–334, August 1991.

39. Oksanen, M. I., P. K. Koivisto, and S. A. Tretyakov, "Vector circuit method applied for chiral slab waveguides," Helsinki University of Technology, Electromagnetics Laboratory Report No. 79, Dec. 1990.

40. Mahmoud, S. F., "Surface wave modes on open chirowaveguides," Abstract in *Proceedings of the 1993 Progress in Electromagnetic Research Symposium,* (PIERS 93), Pasadena, p. 533, July 12–16, 1993.

41. Mahmoud, S. F., "Mode characteristics in chirowaveguides with constant impedance walls," *J. of Electromagnetic Waves and Applications,* Vol. 6, No. 5/6, 625–640, 1992.

42. Oksanen, M. I., P. K. Koivisto, and S. A. Tretyakov, "Plane chiral waveguides with boundary impedance conditions," *Microwave and optical Technology Letters,* Vol. 5, No. 2, 68–72, Feb. 1992.

43. Harrington, R. F., *Time–Harmonic Electromagnetic Fields,* McGraw–Hill, NY, 1961.

44. Engheta, N., and P. Pelet, "Mode orthogonality in chirowaveguides," *IEEE Transactions on Microwave Theory and Techniques,* Vol. MTT–38, No. 11, 1631–1634, November 1990.

45. Walker, L. R., "Orthogonality relations for gyrotropic waveguides," *J. Appl. Phys.,* Vol. 28, No. 3, p. 377, 1957.

46. Pelet, P., and N. Engheta, "Coupled–mode theory for chirowaveguides," *J. of Applied Physics,* Vol. 67, No. 6, 2742–2745, March 1990.

47. Chan, K. S., and P. L. E. Uslenghi, "Chiral rectangular directional coupler," Abstract in *Proc. of the 1991 IEEE AP–S International Symposium/Radio Science Meeting,* Vol. Radio Science Meeting, London, Ontario, p. 362, June 24–28, 1991.

48. Chan, K.-S., and P. L. E. Uslenghi, "Strong coupling between chiral rectangular waveguides," Abstract in *Proc. of the 1992 IEEE AP–S International Symposium/Radio Science Meeting Joint Symposia,* Chicago, Illinois, Vol. URSI Digest, p. 446, July 17–20, 1992.

49. Mazur, J., M. Mrozowski, and M. Okoniewski, "Distributed effects in a pair of parallel guides coupled via a chiral medium and their possible applications," *J. of Electromagnetic Waves and Applications,* Vol. 6, No. 5/6, 641–650, 1992.

50. Cory, H., and T. Tamir, "Coupling processes in circular open chirowaveguides," *IEE Proc. Pt.-H,* Vol. 139, No. 2, 165–170, 1992.

51. Cory, H., and I. Rosenhouse, "Some applications of multilayered chiral structures," *Electronics Letters,* Vol. 28, No. 11, 1051–1053, 1992.

52. Cory, H., and S. Gov, "Mode energy transfer along a circular open chirowaveguide," *Microwave and Optical Technology Letters,* Vol. 6, No. 9, 536–541, 1993.

53. Chein, M., Y. Kim, and H. Grebel, "Mode conversion in optically active and isotropic waveguides," *Optics Letters,* Vol. 14, No. 15, 826–828, 1989.

54. Toscano, A., G. Ungarelli, and L. Vegni, "Characteristics of propagation in the parallel–plate waveguide partially filled with a chiral material," *Proc. of the 1992 IEEE AP-S International Symposium/Radio Science Meeting Joint Symposia,* Chicago, Illinois, Vol. 4 , 2022–2025, July 17–20, 1992.

55. Toscano, A., and L. Vegni, "Effects of chirality admittance on the propagating modes in a parallel–plate Waveguide partially filled with a chiral slab," *Microwave and Optical Technology Letters,* Vol. 6, No. 14, 806–809, 1993.

56. Mahmoud, S. F., "Mode analysis in chirowaveguides with dielectric lining," *Proc. of the 14th Triennial URSI International Symposium on Electromagnetic Theory,* Sydney, Australia, August 17–20, 1992. See also S. F. Mahmoud, "Mode characteristics in chirowaveguides with dielectric lining," *Radio Science,* Vol. 28, No. 5, 929–935, 1993.

57. Saadoun, M. M. I., "The pseudochiral omega (Ω) Medium: Theory and potential applications," Ph.D. Dissertation, Department of Electrical Engineering, University of Pennsylvania, September 1992.

58. Tretyakov, S. A., and A. J. Viitanen, "Waveguide and resonator perturbation techniques for measuring chirality and non-reciprocity of bi-isotropic materials," Helsinki University of Technology, Electromagnetics Laboratory Report No. 134, Feb. 1993.

59. Rong, Y., "Propagation characteristics of circular chirowaveguides periodically loaded with metal gratings," *Proceedings of the IEE, Part H,* Vol. 140, No. 4, 254–258, 1993.

60. Mariotte, F., and N. Engheta, "Reflection and transmission of guided electromagnetic waves at an air–chiral interface and at a chiral slab in a parallel–plate waveguide," *IEEE Trans. Microwave Theory and Techniques,* Vol. MTT–41, No. 11, 1895–1906, 1993.

61. Mariotte, F., and N. Engheta, "Reflection from a lossy chiral slab (with or without metallis backing) in a parallel–plate waveguide," submitted to *Radio Science.*

62. Bassiri, S., C. H. Papas, and N. Engheta, "Electromagnetic wave propagation through a dielectric–chiral interface and through a chiral slab," *J. Opt. Soc. Am. A.,* Vol. 5, No. 9, 1450–1459, 1988.

63. Pelet, P., and N. Engheta, "Novel rotational characteristics of radiation pattern of chirostrip dipole Antennas," *Microwave and Optical Technology Letters,* Vol. 5, No. 1, 31–34, January 1992.

64. Hollinger, R. D., V. V. Varadan, D. K. Ghodgaonkar, and V. K. Varadan, "Experimental characterization of isotropic chiral composites in circular waveguides," *Radio Science,* Vol. 27, No. 2, 161–168, March–April 1992.

65. Kao, T.-T., and P. L. E. Uslenghi, "Theory of measurement of the constitutive parameters of certain magnetoelectric media," Abstract in *Proc. of the 1992 IEEE AP–S International Symposium/Radio Science Meeting Joint Symposia,* Chicago, Illinois, Vol. 4 , p. 2260, July 17–20, 1992.

66. Uslenghi, P. L. E., "Theory of certain bi–anisotropic Waveguides," *Proc. of the 14th Triennial URSI International Symposium on Electromagnetic Theory,* Sydney, Australia, August 17–20, 1992.

67. Paiva, C. R., and A. M. Barbosa, "A method for the analysis of bi-isotropic planar waveguides: application to a grounded chiroslabguide," *Electromagnetics,* Vol. 11, 209–221, 1991.

68. Paiva, C. R., and A. M. Barbosa, "Linear–operator formulation for the analysis of inhomogeneous bi-isotropic planar waveguides," *IEEE Trans. Microwave Theory and Techniques,* Vol. 40, No. 4, 672–678, April 1992.

69. Viitanen, A. J., and I. V. Lindell, "Perturbation theory for a corrugated waveguide with a bi-isotropic rod," *Microwave and Optical Technology Letters,* Vol. 5, No. 14, 729–732, Dec. 1992.

70. Mazur, J., "Non-reciprocal phenomena in coupled guides filled with chiroferrite media," *J. of Electromagnetic Waves and Applications,* Vol. 7, No. 10, 1395–1415, 1993.